Real-time resource model updating for improved coal quality control using online data

Yüksel, Cansin; Thielemann, T; Wambeke, Tom; Benndorf, Joerg

DOI
10.1016/j.coal.2016.05.014

Publication date
2016

Document Version
Accepted author manuscript

Published in
International Journal of Coal Geology

Real-Time Resource Model Updating for Improved Coal Quality Control Using Online Data

C. Yüksel [1], T. Thielemann [2], T. Wambeke [3,4], J. Benndorf [5]

[1,3,5] *Resource Engineering Section, Department of Geoscience & Engineering, Delft University of Technology, Delft, Netherlands*

[2] *RWE Power AG, Stüttgenweg 2, 50935 Köln, Germany*

[4] *MTI Holland - Royal IHC, the Netherlands*

Abstract

In recent years a real-time resource model updating concept has proven to increase the material quality control and process efficiency in geostatistics. The real-time resource model updating concept integrates online-sensor data, measured from the production line, into the resource model. This integration quickly improves the accuracy of the resource model. The aim of this contribution is to adapt this concept into coal production and to apply the developed framework on an industrial case. The result of this study will provide an additional improvement to coal quality management, by mainly focusing on the ash content in the deposit. This includes high ash values in coal seams, which are caused by sand intrusions and are greatly affecting the operational process. A tailored Ensemble Kalman Filter approach, specifically applicable in coal production, is presented after a detailed literature review. For validation, a 2D case study is performed in a fully controllable environment. Further, the approach is benchmarked against an alternative proven approach. To demonstrate the value added a full scale industrial application is performed focusing on improving the lignite quality control in the production process. The results of integrating online measurement data into the resource model indicate a significant improvement (in the order of 70%) in coal quality production.

Keywords: Ensemble Kalman filter, coal mining, resource management, resource model, online-sensor data, industrial application

[1] Corresponding Author: Address: Room 3.31, Stevinweg 1, 2628 CN, Delft, Netherlands.
Mobile: +31 6 87 65 45 51, Tel: +31 15 27 89 995
Email: C.Yuksel@tudelft.nl

1 Introduction

In mining, modelling of the deposit geology is the basis for many actions to be taken in the future, such as predictions of quality attributes, mineral resources and ore reserves, as well as mine design and long-term production planning. The essential knowledge about the raw material product is based on this prediction, which comes with some degree of uncertainty. This uncertainty causes one of the most common problems in the mining industry, predictions on a small scale such as a train load or daily production are exhibiting strong deviations from reality.

Some of the most important challenges faced by the lignite mining industry are marine and fluvial sand intrusions located in the lignite deposit. These intrusions are translated in the coal seams as the high ash values (e.g. more than 15% ash). Most of the times, these high ash values cannot be captured completely by exploration data and in the predicted deposit models. This lack of information affects the operational process significantly.

The current way of predicting the coal quality attributes is using geostatistical interpolation or simulation to create resource models based on exploration data, which are very precise but separated by large distances. Mining companies have lately started to benefit from the recent developments in information technology, including online-sensor technologies for the characterization of materials, measuring the equipment efficiencies or defining the location of the equipment. KOLA (an abbreviation for Kohle OnLine Analytics) and RGI (radiometric measuring system) online-sensor measurements are two different sensor measurement systems that are recently used for assessing the components of the produced lignite. The precision of the data is lower than exploration data, which are analysed in laboratories. However, these data are much more dense than exploration data and provide additional information about the coal seam.

To benefit from this available dense data, a close loop concept for mining has recently been introduced (Benndorf et al., 2015). A new algorithmic approach was created because of the necessity to interpret online sensor data fast and near-real time in contrary to traditional methods. In lignite mining, reconciliation exercises are done regularly, however due to the nature of laboratory analysis, the exercises take days or weeks. The concept offers to combine the measured sensor data into the resource model by using sequential resource model updating methods that originate from data assimilation.

Simple geostatiscal re-modelling will often not be sufficient, because of the four reasons. The first reason is that the online sensors might be measuring blended material originating from different benches/blocks. In this case, tracking the material quality with geostatiscal re-modelling might not be possible. The second reason is that the quality of the online sensor data might require co-simulation procedures, however these procedures create additional work. The third reason is the change of support, due to measuring a small amount of material the representativeness of the entire block needs to be calculated. The fourth and most important reason is that linking the measurement with the location of the production block is very difficult, because the measurement location varies. The reasons mentioned above indicate that using geostatiscal methods to integrate the real-time online measurements back into the resource model will be insufficient and difficult. Therefor it was decided to use data assimilation in the developed framework.

Data assimilation methods offer the tools for fast incorporation of observations in order to improve predictions. The definition of data assimilation translates in mining as the process of combining the sensor measurement data with a prior estimation of the resource model, in order to produce a more accurate estimate. Methods of data assimilation have found many successful applications in various fields. With the aim of improved numerical weather forecast, (Bengtsson, Ghil, & Källén, 1981; Daley, 1993; Ghil, Cohn, Tavantzis, Bube, & Isaacson, 1981; Houtekamer & Mitchell, 1998, 2001; Houtekamer et al., 2005) examined and applied different data assimilation methods on dynamic atmospheric models. Applications to oceanographic problems, such as estimation and prediction of ocean eddy fields, wave propagation etc., (Barbieri & Schopf, 1982; Budgell, 1986; Ghil & Malanotte-Rizzoli, 1991; Heemink & Kloosterhuis, 1990; Miller, 1986; Tuan Pham, Verron, & Christine Roubaud, 1998; Verlaan & Heemink, 1997; Webb, 1989) deepened and broadened the understanding of ocean circulation on regional, basin and global scales. Similar to this research, (Bertino, Evensen, & Wackernagel, 2002) successfully combined geostatistics and data assimilation methods and applied it in a estuarine system. More recently in reservoir engineering (Brouwer, Naevdal, Jansen, Vefring, & Van Kruijsdijk, 2004; Nævdal, Johnsen, Aanonsen, & Vefring, 2005; Nævdal, Mannseth, & Vefring, 2002; Sebacher, Hanea, & Heemink, 2013) applied a similar framework of resource model updating approach. The mentioned applications are all performed on nonstationary, dynamical models due the nature of their research fields. The initial difference in application of the resource model updating concept among others comes from the requirement of the stationary, non-dynamic models.

(Benndorf, 2015) has proven the approach to work well within a synthetic case study under a variation of several control parameters (number of excavators, precision of the sensor, update interval, measurement interval, extraction mode/production rate). An extended version of the developed framework includes a Gaussian anamorphosis of grid nodes, sensor-based measurements and model-based predictions; to deal with suboptimal conditions, an integrated parallel updating sequence; to reduce the statistical sampling error without the need of increasing the number of realizations and a neighbourhood search strategy; to constrain computation time and to avoid the spurious correlations, is introduced by (Wambeke & Benndorf, 2015). Yet, so far, the amount of literature is little, particularly when considering the industrial application of the developed concept.

The purpose of this paper is to provide a tailored method, which was adapted to update coal quality attributes in a continuous mining environment, in order to improve the resource model accuracy. Providing more accurate deposit models will lead to an improvement in the detection of sand intrusions in future production areas. As a result, this approach will allow quicker reactions to gained knowledge, which in turn allows quick changes in mine planning and operational decisions.

The research questions driving this study are as follows:

- Is it possible to update the coal quality attributes, namely the ash contents, by using data assimilation methods, which have so far mainly been applied other contents, in order to improve the resource model accuracy and mine planning?
- Is the defined updating framework applicable for a full scale lignite production environment?

The findings of this research are expected to assist the operational decision making in lignite production and improve the future applications of the resource model updating concept.

The remainder of the article is structured as follows: First, the geological formation of the lignite seams and the development of the sand intrusions in Garzweiler mine are provided in

order to explain the intrusions from a geological perspective. Thereafter, current online-sensor measurement technology information is given. Next, the principles behind the resource model updating framework developed for a specific application in continuous mining and the mathematical formulation, are presented. For verification, a 2D case study in a fully controllable environment and it's validation study are illustrated. Findings of the study are then presented. This is followed by an industrial application in Garzweiler mine, Germany. Results are discussed and summarised. The article concludes with a summary of the research contributions and directions for the future research.

2 Geology and the Available Sensor Data

This chapter explains the geological formation of the lignite seams and introduces the development of the main problem caused by the sand intrusions in Garzweiler mine. Next, the available sensor data are presented in order to guide the reader towards the solution.

2.1 Geological Formation of the Lignite Seams

In Tertiary (Oligocene) times, the subsidence of the Central Graben in the North Sea created the Lower Rhine Embayment (LRE) as southernmost extension of the Central Graben (Klostermann, 1991). A new sedimentary basin was created. The LRE contains up to 1,600 m of these Oligocene to Pleistocene siliciclastic sediments with intercalated lignite attaining a thickness of up to 100 m (Hager, 1986). The lignite is of considerable economic importance and has been exploited in open cast mines and near-surface operations since the 18th century, at locations where the seams were easily accessible (Schäfer, Utescher, Klett, & Valdivia-Manchego, 2005). Since then, the exploitation of the coal by RWE Generation SE - formerly Rheinbraun AG – is forming a vital basis of German power supply.

Sedimentation in the LRE was mainly influenced by fault block tectonics and variations in sea level. In Upper Oligocene, a 70 Ma long phase of high sea levels came to an end. Short term sea level fluctuations became typical (Haq, Hardenbol, & Vail, 1987). As a consequence, sequences of marine sands (representing a sea level high) intercalated with terrestrial silts, clays and lignite seams (sea level low) were sedimented. 18 Ma ago, in lower Miocene times (Burdigalian) the uplift of the surrounding highlands named "Rhenish Schiefergebirge" relative to its foreland slowed down. This decreased the sedimentary flows being accumulated in the LRE. At the same time, the climate warmed up. The temperature of North Sea shallow waters rose to 16 °C (Buchardt, 1978). Higher precipitation led to a subtropical climate and rising groundwater tables (Zagwijn & Hager, 1987). Vegetation could gain ground extensively and left behind peat, which gradually was converted into lignite.

The place of this research area, the mine Garzweiler, was part of the Venlo block. During two marine regressions, 17 and 15 Ma ago, the deposition of the later lignite seams Morken (named 6A after (Schneider & Thiele, 1965)) and Frimmersdorf (named 6C) took place. They were separated by the marine Frimmersdorf sands (named 6B). Additionally, as the area of the mine Garzweiler was close to the shore line during that period, the seam Frimmersdorf (6C) faced numerous marine sand intrusions. These irregular sand partings within 6C and their predictability are part of this research project described here. On top of the seam 6C, the marine Neurath sands (named 6D) were sedimented similar to today's Wadden Sea sedimentation. On top, the seam Garzweiler (6E) was formed during a period of marine regression. In upper Miocene times, the climate cooled down gradually and the LRE underwent a faster downlift. This enhanced the downward gradient and enforced the competence of rivers from the South. Thick fluvial and limnic sediments were deposited,

named horizons 7 and 8 after (Schneider & Thiele, 1965). Their clastic burden led to an easy consolidation of the peat to form lignite.

2.2 Development of Sand Intrusions in Seam 6C, Mine Garzweiler

The Garzweiler open cast mine is located west of Grevenbroich and is moving westward in the direction of Erkelenz. The mine mainly touches Rhein county Neuss, Rhein-Erft county and Heinsberg county. The lignite is deposited in three seams which together are 40 m thick on average. The coal lays some 40 to max 210 m below the earth's surface.

The Frimmersdorf lignite seam 6C contains multiple sand intrusions. The shape and size of these sand partings are irregular and both characteristics are showing a large variability. However, there is not a common idea about the origin of the sand partings. Several possible scenarios for their origin are shortly described below. The first three scenarios are describing a syn-sedimentary process, as opposed to the fourth scenario, which describes a post-sedimentary process:

1. An environment of marine transgression

   A rising sea level led to relatively homogeneous sand bodies in the peat. This marine environment arose slowly. Hence, sand partings developed over a longer period of time.
2. Accidental injection of heterogeneous sand bodies

   Rough weather and wild sea conditions could accidentally inject a volume of sand within the peat. These events can happen quickly; a daily or hourly event may suffice. Currently, these kinds of events are seen at the German coast near Wilhelmshaven.
3. An environment of marine regression and increasing fluvial impact

   A decreasing sea level could strengthen the impact of fluvial conditions. "Crevasse splay" - a situation of a broken embankment causing flooding in the adjacent swampy area - could lead to sand partings within the lignite.
4. Coalification

   The geochemical process of coalification can be simplified by the following equation:
   peat + water + CO_2 = lignite
   Here, incidental CO_2 release could be accompanied by large volume relocation. This event could remobilize 6C sand or cause an intrusion of 6D sand into the 6C lignite.

To better predict the quality of lignite to be produced, the genesis of sand partings is rather of second importance. For an improved coal quality control, more important is the combination of data of the existing geological model with production data, GPS data of the excavator’s position at one time and data of analytical results of the coal composition. The theoretical formulization of the mentioned data fusion is provided in Chapter 3. Application of this fusion in the Frimmersdorf lignite seam will be provided in Chapter 4.

2.3 Available Sensor Data

There are two different online-sensor measurement systems that are available in RWE to characterize the lignite produced from the Frimmersdorf seam.

The KOLA - an abbreviation for Kohle OnLine Analytics - system is the first data type available for a more extensive modeling of the sand parting in the 6C Frimmersdorf lignite seam. It applies X-Ray diffraction in order to accurately assess the components of the produced lignite. The analyzed components are inter alia iron, sulfur, potassium, calcium and - of importance in the context of this research - the ash content of the produced lignite. The

Garzweiler opencast mine operates multiple KOLA measuring stations, of which two are analyzing the coal from the Frimmersdorf lignite seam.

The second available source is the radiometric measuring system of RGI data. This system allows an online determination of the ash content of the mass flow directly on the conveyor belt, without requiring any sampling or sample processing. It is installed directly on the excavator that produces lignite from the Frimmersdorf seam and, consequently, the ash content of the produced lignite can be provided by online values during the process of monitoring and controlling the production process. However, calibration of this system is strongly dependent on the composition of the coal.

The presented full case study in Chapter 4 only used the KOLA measurement data as the representative measurement of the produced lignite due to the calibration problems of the RGI measurements.

3 A Method for Updating Coal Attributes in a Short-Term Model Based on Online-Sensor Data

This chapter provides the theoretical background of the adopted algorithmic approach in order to fully utilise available online data to improve prediction of (sand intrusion related) ash content. A formal description of the updating algorithm is provided in section 3.1. Thereafter a 2D case study in a fully known environment is illustrated in section 3.2. To conclude this chapter, section 3.3 presents a benchmark of the method against an alternative proven approach.

In lignite mining, similar to other branches of mining, the initial step, prior to mining activities, is creating a resource model based on exploration data, such as drill hole data. Traditionally in order to produce a valuable representation of the coal seam geometry and quality attributes of the seam, such as ash content, the geostatistical interpolation methods are used. Based on this resource model, a short-term production plan is created and mining activities will be executed according to this plan. In case of discovering unexpected waste intrusions in the coal seam during production, the short-term model has to be renewed. Currently, by using off-line analysis and modelling techniques, this may take days or sometimes even weeks. Using online-sensor techniques for coal quality characterisation in combination with rapid resource model updating, a faster reaction to the unexpected deviations can be implemented during operations, leading to increased production efficiency. This concept was initially proposed by (Benndorf et al., 2015) as a closed loop framework. Figure 1 illustrates this conceptual workflow that basically integrates the online-sensor data into the resource model, as soon as they are obtained.

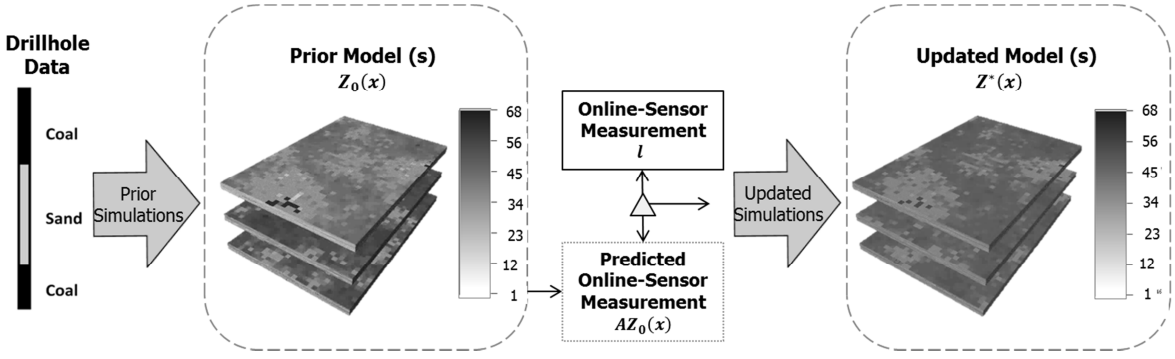

Figure 1 An overview of the EnKF based resource model updating concept

Predicting the initial resource model, so-called prior model, is traditionally done by Kriging. Kriging provides the best estimate which is close to reality, yet it is much smoother and doesn't represent the in-situ variability fully. For this reason, it is essential to model the spatial uncertainty by generating multiple realizations of the joint distribution of the ash values in seam using stochastic simulation. Sequential Gaussian simulation (SGS) is a very efficient method for risk assessment applications in the mining industry.

The method compares the predicted measurement values based on the prior prediction (realizations) and the actual online-sensor measurement values per produced block. Once prior models are available, predicted measurement values are required to be calculated according to the production sequence, based on prior predictions. The difference between this predicted measurement value and the actual online-sensor measured value per produced block will be fed back to the resource model, in order to create the updated resource model, the so-called posterior model (Figure 1). It is important to mention that in general, sensor measurements will have an error component.

For rapid updating of the resource model, sequentially observed data have to be integrated with prediction models in an efficient way. In related fields, methods of data assimilation found many successful applications.

Data assimilation can be defined as the fusion of observations into the prior knowledge (e.g. estimation, simulations) in order to improve the predictions. Thus, this definition translates in mining as the process of combining online-sensor measurement data with the prior model to produce a more accurate prediction of the resource model, the so-called posterior model.

Sequential data assimilation methods use a probabilistic framework and give estimates of the whole system state sequentially, by propagating information only forward in time (Bertino, Evensen, & Wackernagel, 2003). The main sequential methods are the Kalman Filter (KF) (Kalman, 1960) (Kalman and Bucy, 1961) and the various filters that have been derived from the basis of the KF, such as; the extended Kalman filter (EKF), the ensemble Kalman filter (EnKF) (Burgers, Jan van Leeuwen, & Evensen, 1998; Evensen, 1994, 1997a, 1997b; Evensen & Van Leeuwen, 1996, 2000), the ensemble transform Kalman filter (ETKF) (Bishop, Etherton, & Majumdar, 2001) and the ensemble square root filter (EnSRF) (Whitaker and Hamill, 2002).

The (KF) is an optimal recursive data assimilation method that combines all available data, such as prior knowledge about the system and measurements, in order to produce an estimate of the desired variables in such a manner that the error rate is minimized statistically. The KF works in two stages. The first stage solves forecast equations, where the prior knowledge is represented by a model to the time of an observation. In our case, it is not necessary to use this part of the filter since the prior model is created through estimation and simulation. The second stage is the "sequential updating" stage, where the online-sensor measurements are assimilated into the prior model. This is done according to a ratio of errors in the prior model and in the observations. The difference between the sensor measurements and the predicted measurements is multiplied by a weighting factor (based on the mentioned ratio of errors) and this weighted difference is added to the prior model. An updated resource model is then produced. A detailed explanation on Kalman Filter is given in (Maybeck, 1979), (Stengel, 1994) and (Cohn, 1997), the following will focus on the application of the Kalman filter in geosciences.

A framework with a similar aim has been recently proposed by (Chevalier, Emery, & Ginsbourger, 2014) to update the conditional simulations at minimal cost. The formulae offers significant computational savings when the number of conditioning observations is

large, and quantifies the effect of the newly assimilated observations on already simulated sample paths. Yet, the application of this method in resource model updating using online data case would not be as efficient since the change of support technique is not taken account. In coal production, the obtained quality measurements represent only a small ratio of the entire production block. For this reason, it is essential to apply change of support methods in order to correct the online-sensor measurements in a way to represent a whole production block.

3.1 A Formal Description of the Updating Algorithm

The developed framework based on KF is initially validated on the estimated prior model then it is extended to use the SGS method for creating realizations of the prior model.

Let $\boldsymbol{Z}(\boldsymbol{x})$ be the state of a stochastic process modelling the spatial distribution, where $\boldsymbol{Z}$ refers the local ash content at excavation locations $\boldsymbol{x}$, then the updated resource model, $\boldsymbol{Z}^*(\boldsymbol{x})$, is calculated by the following equation:

$$\boldsymbol{Z}^*(\boldsymbol{x}) = \boldsymbol{Z_0}(\boldsymbol{x}) + \boldsymbol{K}(\boldsymbol{l} - \boldsymbol{A}\boldsymbol{Z_0}(\boldsymbol{x})) \quad (1)$$

where $\boldsymbol{Z_0}(\boldsymbol{x})$ is the prior resource model, $\boldsymbol{l}$ is sensor based measurements, $\boldsymbol{A}$ represents the production sequence matrix, so the term $\boldsymbol{A}\boldsymbol{Z_0}(\boldsymbol{x})$ represents the predicted measurements based on the prior block model. Matrix $\boldsymbol{A}$ describes the contribution of each of the mining blocks at $\boldsymbol{x_i}$ to the total production at a certain time interval $\boldsymbol{t_j}$, with j = 1, … , m

$$\boldsymbol{A} = \begin{bmatrix} a_{1,1} & \cdots & a_{1,m} \\ \vdots & \ddots & \vdots \\ a_{n,1} & \cdots & a_{n,m} \end{bmatrix}. \quad (2)$$

The elements $a_{i,j}$, can be interpreted as contributions of each mining block *i* to the produced material being on the conveyor belt, which will be eventually observed at some sensor station at time *j*. Matrix $\boldsymbol{A}$ is herein called production matrix and can be interpreted as an observation model, which links the block model $\boldsymbol{Z}(\boldsymbol{x})$ with sensor observations.

The Kalman gain, $\boldsymbol{K}$**,** calculates a weighting factor based on the prediction and measurement error covariances. The Kalman gain matrix indicates the reliability of the measurements, this is done in order to decide “how much to change the prior model by a given measurement” and can be derived from a minimum variance estimate, which leads to the KF providing an optimal solution by minimising the cost function.

$$\boldsymbol{K} = (\boldsymbol{A}^T\boldsymbol{C_{zz}}\boldsymbol{A} + \boldsymbol{C_{ll}})^{-1}\boldsymbol{A}^T\boldsymbol{C_{zz}} \; . \quad (3)$$

Kalman gain can be calculated as in Equation (3). As mentioned above, it contains two different error sources, $\boldsymbol{C_{zz}}$, the model prediction error and $\boldsymbol{C_{ll}}$, the measurement error. The model prediction error is basically the covariance matrix of the prior resource model, which is propagated through the lignite mining by the production sequence matrix $\boldsymbol{A}$. The measurement error is the covariance matrix of the sensor-based measurement. The term $\boldsymbol{A}^T\boldsymbol{C_{zz}}$ in Equation (3) denotes the model-based prediction, as previously defined.

$$\boldsymbol{C_{zz}}^* = (\boldsymbol{I} - \boldsymbol{K}\boldsymbol{A})\boldsymbol{C_{zz}} \quad (4)$$

The improvement in model prediction can be determined as the updated model error covariance, $\boldsymbol{C_{zz}}^*$, which is provided in Equation (4). Clearly, this leads to a decrease in the uncertainty of the resource model blocks, not only for the currently excavated ones but also for the adjacent blocks which are spatially correlated. Figure 2 illustrates an overview of the KF based resource model updating concept.

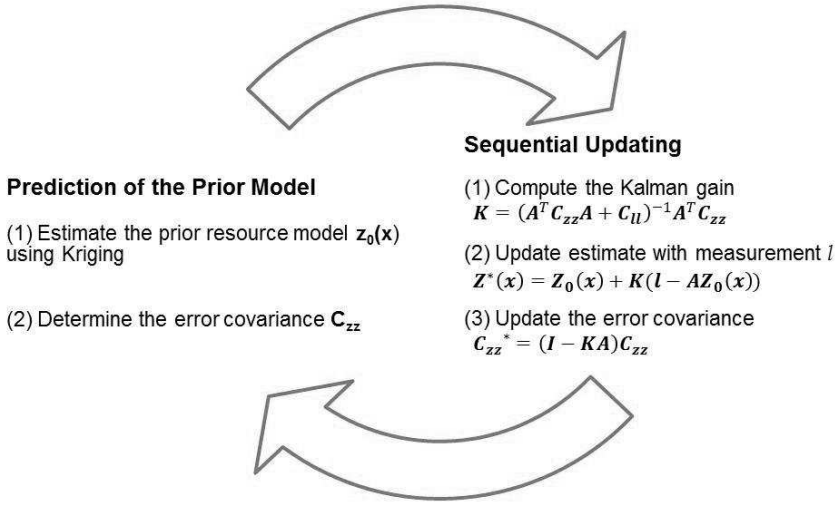

Figure 2 An overview of the KF based resource model updating concept

It is obvious that the KF offers large potential in improving resource recovery by combining online data with the resource model and consequently decreasing its uncertainty. However, there are different challenges to solve in order to comprehend the source of the difference between sensor measurement and the resource model, and feed the gained knowledge back to the resource model. The main challenges to solve are the size of the estimated resource model (in the order of multiple millions of grid nodes), non-Gaussian behaviour of data, the different support of observations and resource model blocks and a possible non-linear relationship between the observations and model attributes.

The (EnKF) provides a comprehensive solution for large-scale applications when explicit storage and manipulation of the covariance matrix is impossible or not feasible (Sakov & Bertino, 2011). Moreover, EnKF is able to deal with the non-linear systems. The developed framework with ENKF uses SGS in order to create the ensemble of realizations, also called prior ensemble $\boldsymbol{Z_0(x)}^e$, where $e = 1, \dots, N$ is the number of realizations/ensembles. Next, the algorithm continues recursively, using the following recurrence relations;

$$\boldsymbol{Z^*(x)}^e = \boldsymbol{Z_0(x)}^e + \boldsymbol{K}^e(\boldsymbol{l}^e - \boldsymbol{AZ_0(x)}^e) \ . \quad (5)$$

$$\boldsymbol{K}^e = (\boldsymbol{A}^T \boldsymbol{C_{zz}}^e \boldsymbol{A} + \boldsymbol{C_{ll}}^e)^{-1} \boldsymbol{A}^T \boldsymbol{C_{zz}}^e \quad (6)$$

$$\boldsymbol{C_{zz}}^{*e} = \overline{(\boldsymbol{Z(x)}^e - \overline{\boldsymbol{Z(x)}^e})(\boldsymbol{Z(x)}^e - \overline{\boldsymbol{Z(x)}^e})^T} \quad (7)$$

where $\boldsymbol{Z(x)}^e$ and $\boldsymbol{l}^e$ respectively consist of an ensemble of block models and the measurements. In Equation (7) $\boldsymbol{C_{zz}}^{*e}$ refers to the updated error covariance of the resource model, where the overbar denotes the expected values of the ensembles. The covariance matrices represent the whole ensemble and the Kalman gain $\boldsymbol{K}^e$ is derived from these.

Two measures are implemented to reduce computational time of Kalman gain (Wambeke & Benndorf, 2015). The first measure is related to the neighbourhood. The size of the $\boldsymbol{C_{zz}}$ matrix is in the order of the size of the blocks that are in the defined updating neighbourhood. The second measure is a Cholesky decomposition which is implemented to avoid an explicit computation of the inverse in Equation 6. This results significant computational speed ups.

To deal with the non-gaussianity of the data, a new approach NS-EnKF is proposed by Zhou (Zhou, Gómez-Hernández, Hendricks Franssen, & Li, 2011) which transforms the original

state vector into a new vector that is univariate Gaussian at all times. Gaussianity is achieved by applying a normal-score transformation to each variable for all locations and all time steps, prior to performing the updating step in EnKF.

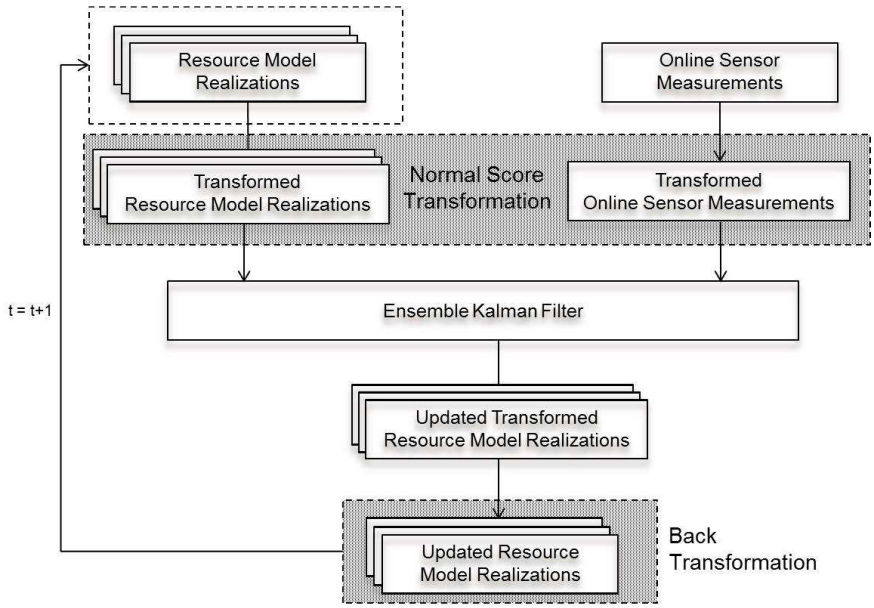

Figure 3 Real-time updating algorithm based on NS-EnKF approach, modified from (Zhou et al., 2011)

The NS-EnKF approach follows the same steps as the standard EnKF, except the NS-EnKF has additional pre and post processing steps. Local grades at grid nodes will be normal score transformed before application of the EnKF, and once the update is complete, the normal score transformed data will be transformed back (Figure 3). Readers are referred to (Goovaerts, 1997) for information about the normal score transformation.

With the goal of a continuously updatable coal quality attributes in a resource model, a framework based on the NS-EnKF approach was tailored for large scaled mining applications. It is based on an implementation from (Wambeke & Benndorf, 2016). Figure 4 gives general overview of the operations which are performed to real-time resource model updating for improving the coal quality control using online data. The concept initially starts with resource modelling by using a geostatistical simulation technique, namely sequential Gaussian simulation (SGS). This is the first required data set. The second data set consists of a collection of actual and predicted sensor measurements. The actual online-sensor measurement values are collected during the lignite production and the predicted measurements are obtained by applying the production sequence on the prior resource model realizations. Once both of the input data are provided into the NS-EnKF approach based real-time updating framework, the updated posterior resource model will be obtained. This process will continue as long as the online-sensor measurement data is received.

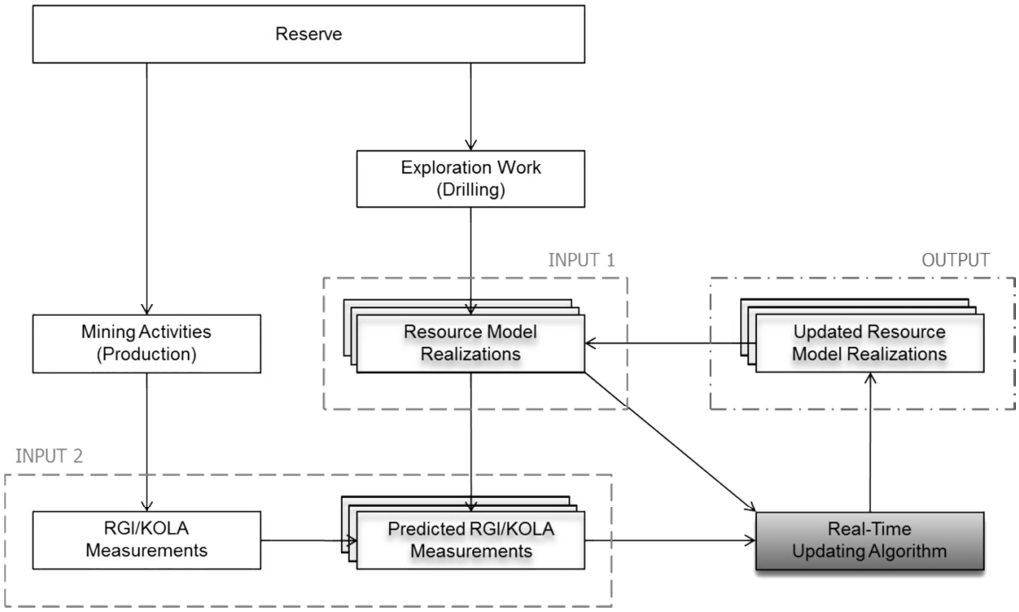

Figure 4 Configuration of the real-time resource model updating concept, modified from (Wambeke & Benndorf, 2016)

3.2 A 2D Case Study

The aim of this 2D case study is to investigate the capability of the introduced concept in real-time update on a resource model and to obtain more accurate resource models for future processes. This section will describe the set-up of the experiments, explain some details about performance measures and finally, provide the results of the case studies.

3.2.1 Experiment Set-Up

All of the experiments presented in this section are performed in a completely known and fully controllable environment; a well-known geostatistical dataset, called *Walker Lake* dataset (Isaaks & Srivastava, 1989). The dataset originally contained digital elevation data from the Walker Lake area (California-Nevada border), in our case those will be interpreted as the concentration values.

Realizations of the block model are created by conditional simulation. The blocks were defined with a dimension of 16m x 16m x 10m. The density is assumed 2 t/m^3 , which leads a tonnage of 5120t for one mining block.

No availability of sensor data require generation of new virtual sensor data. The artificial sensor data are composed of three components. Component one is the true block grade taken from the exhaustively known data set. Component two captures the volume variance relationship and corrects the block value support to a smaller measured support by adding the corresponding dispersion variance (Isaaks & Srivastava, 1989; Krige, 1951, 1981). The third component represents the precision of the sensor and, for this case study, varies between 1, 5 and 10%.

It is assumed that the excavated material is discharged on a non-stationary conveyor belt positioned on the benches in the mining area. The conveyor belts then combine the material flow at the central mass distribution point. The combined material flow is scanned by a sensor positioned above the conveyor belt.

The mining system consists out of, either one, two, three or four bucket-wheel excavators positioned at different benches with different digging rates. In the case of one excavator, the

mine design assumes that the excavation starts from the south-west corner of the block model and continues through the east direction until the entire row is mined (Figure 5). When the excavation of the first row is completed, the excavator moves to the northern row and continues to excavating in a western direction. In case of two excavators, the second excavator starts at the south-eastern corner of the northern half of the field. In the case of three and four excavators, the field is divided in three and four parts respectively.

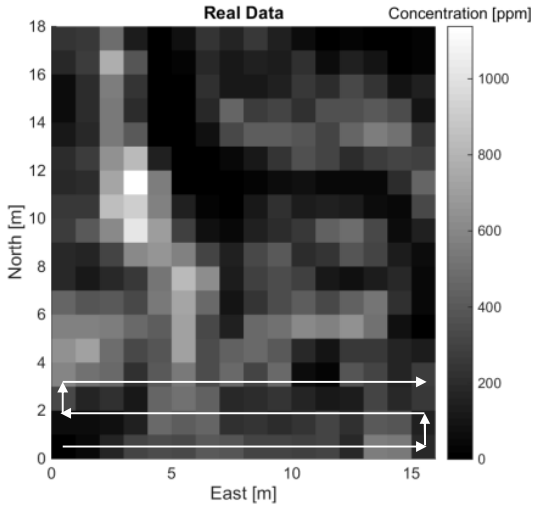

Figure 5 Mining sequence

3.2.2 Results and Discussion

A series of experiments is performed in order to analyse the performance of the updating concept. This section provides some representative results from the performed experiments. Three different performance measures are used in order to present results of the performed experiments.

The first measure is an empirical error measure so called mean square difference, or mean square error (MSE). MSE compares the difference between estimated block value $\boldsymbol{Z}^*(\boldsymbol{x})$ and real block value $Z(\boldsymbol{x})$ from the exhaustive data set and it can be calculated as follows:

$$MSE = \frac{1}{N}\sum_{i=1}^{N}(\boldsymbol{z}^*(\boldsymbol{x_i}) - \boldsymbol{z}(\boldsymbol{x_i}))^2 \quad (8)$$

The second measure is the theoretical block variance (BV), which can be approximated by the EnKF Equation (7) or:

$$BV \cong \frac{1}{N}\sum_{i=1}^{N}\left(\left(\boldsymbol{z}(\boldsymbol{x_i}) - \overline{z(\boldsymbol{x})}\right)\left(z(\boldsymbol{x_i}) - \overline{z(\boldsymbol{x})}\right)^T\right) \quad (9)$$

Both of the mean square error and block variance bar plots are illustrated relative to the prior model in order to make a good comparison. Each plot contains four bars, from left to right; prior model, mined blocks, adjacent blocks and indirect blocks (two blocks away).

Table 1 MSE and BV plots – 2D Case Study

	Mined Blocks	Adjacent Blocks	Indirect Blocks
MSE	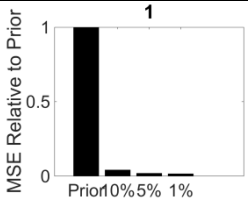	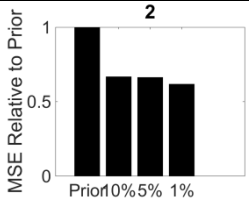	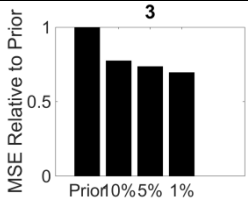

BV	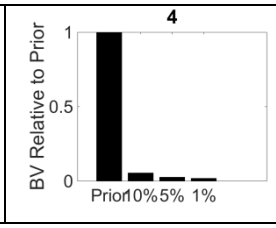	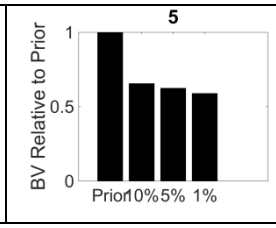	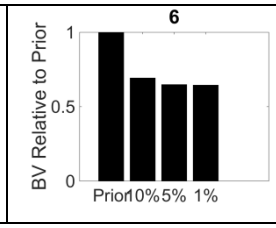

Table 1 gives the MSE and BV plots. The graphs are obtained under the following conditions: one excavator was operating, undergoing measurements every 10 minutes and updating the resource model every hour. The following observations can be made based on the graphs given in Table 1:

- For mined blocks, the uncertainty almost vanishes while the sensor error decreases. This is expected because in case of one excavator the sensor measurements can be clearly tracked back to the source block. Residual uncertainties can be caused by the sensor precision and also interpreted as the limit of the filter for this special application.
- Adjacent blocks are updated resulting in a significant improvement compared to the prior model. This improvement is due to the positive covariance between two adjacent blocks. In addition, the sensor precision effect can be observed from the results.
- Blocks in the second next row are still updated. As expected, the error in prediction increases when moving further away from the point of measurement (from mined block, to adjacent and indirect blocks).

Finally, the third measure is a representative map of the study area which indicates the differences between the real value and updated values of the area (Figure 6).

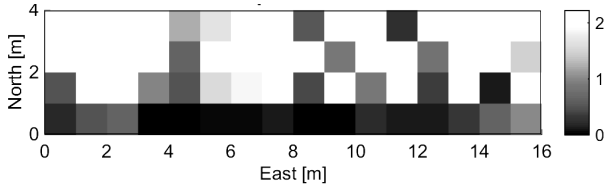

Figure 6 Difference map between the real data and updated model on 50th simulation.

The experiment was designed to update only the blocks in the first row, by integrating their relative measurements. Figure 6 indicates almost no difference between reality and the updated model. In the second row, it is still possible to observe the updates by investigating the small differences between reality and the updated models. Once again, the difference maps prove that the developed framework is suitable for this specific application.

Results show the validity of the real-time resource model updating concept in a 2D scale. The consistency gets reduced when the update moves from mined blocks to indirect blocks, as is expected.

3.3 Validation of the Developed Framework

Results in the previous section indicated a significant level of improvement in the resource models by incorporating sensor data. A reduction of uncertainty is observed after the data assimilation. In order to continue, the method is benchmarked against a proven and well-studied, however computationally expensive method of rejection sampling.

The rejection sampling method is chosen for validation purposes due to its simplicity. Similar applications of this method can also be found in reservoir engineering (Barker, Cuypers, & Holden, 2000; Hegstad & Henning, 2001; Liu, Betancourt, & Oliver, 2001; Liu & Oliver, 2003). Rejection sampling is a Monte Carlo method that proposes a sample from some relatively simple distribution, after which a test is applied to decide whether or not to accept it. It is based on the fact that the posterior is a subset of the prior distribution, and therefore it can be evaluated by sub-sampling the prior (Jeong, Mukerji, & Mariethoz, 2011). All accepted samples are truly independent since the accept/reject criteria do not depend on the most recent sample.

To implement this method, 1000 realizations were created by using a Sequential Gaussian Simulation method, the so called prior models. The developed updating framework was applied to the 1000 prior models in order to generate 1000 updated realizations (updated posterior models). As the rejection sampling proposes that the posterior is a subset of the prior distribution, it is expected that one can obtain the updated posterior distributions by applying rejection sampling to our prior models.

To generate realizations from the target probability density $f(m)$, we let $h(m)$ be a probability density of one single realization and suppose that there is some constant c such as $f(m) \leq ch(m)$ for all m.

To obtain random realizations from $f(m)$:

1. Select a candidate realization (from 1000 prior models) $m*$ from pdf $h(.)$,
2. Generate a decision variable u from $U(0, ch(m*))$,
3. If $u \leq f(m*)$ then accept the proposed model, return $m = m*$. Else, reject the proposed model $m*$ and stay at the current model.
4. Return to step 1 for the next realization.

The conditional probability density $f(m)$ is provided by Bayes rule and can be calculated as follows,

$$f_{(M|D)(m|d_{obs})} = f_{(D|M)(d_{obs}|m)} f_M(m) \Big/ \int f_{(D|M)(d_{obs}|m)} f_M(m)\, dm \tag{10}$$

$$\propto \exp\left(-\frac{1}{2}(\boldsymbol{AZ_0}(x) - \boldsymbol{l})^T \boldsymbol{C_{ll}^{-1}} (\boldsymbol{AZ_0}(x) - \boldsymbol{l})\right) x \exp\left(-\frac{1}{2}(\boldsymbol{Z_0}(x) - \boldsymbol{\mu})^T \boldsymbol{C_{zz}^{-1}} (\boldsymbol{Z_0}(x) - \boldsymbol{\mu})\right) \tag{11}$$

where $\boldsymbol{AZ_0}(x)$ is the predicted observation and $\boldsymbol{Z_0}(x)$ is the prior model and $\boldsymbol{\mu}$ is the mean value of the prior model. $\boldsymbol{C_{ll}}$ and $\boldsymbol{C_{zz}}$ are the measurement error covariance and the prior model covariance respectively.

Figure 7 illustrates the performed experimental scheme. The given algorithm is applied to both 1000 prior models and 1000 updated posterior models. Around 290 of 1000 prior models were accepted, while 950 of 1000 updated posterior models were accepted. The fact that almost all of the updated posterior models are accepted shows a significant improvement over the prior models (from 29% to a 95% acceptance rate). This indicates that the updated posterior models are closer to reality than the prior models.

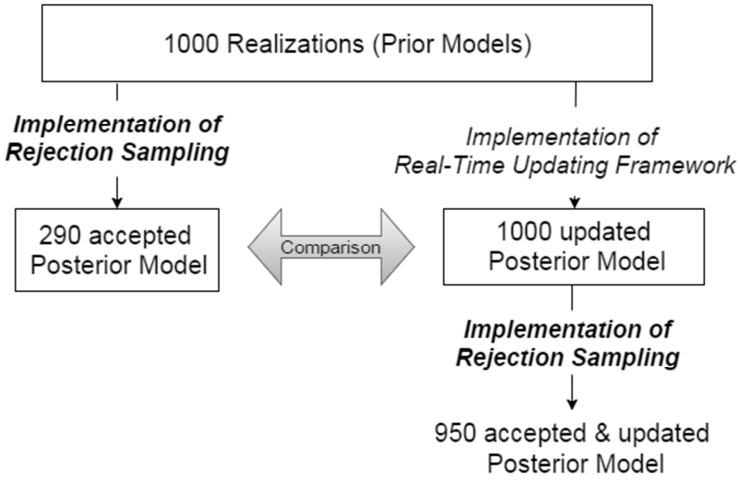

Figure 7 Validation experiment scheme

The 290 accepted posterior models and 1000 updated posterior models are compared to each other in order to investigate the similarities. Therefore, the average of mean and variance of the distributions are compared.

Figure 8 and Figure 9 show the average of mean and variance of the posterior models obtained from rejection sampling and updating framework, respectively. It is clearly seen that the average mean and variance of accepted prior models (290) and updated prior models (1000) are very similar to each other. Figure 10 is provided for a better comparison between the accepted posterior realizations from rejection sampling (290) and updated posterior realizations from the real-time update framework (1000). The deviations between two models are very small. One can conclude that the updated posterior realizations from the real-time update framework are reproduced through rejection sampling.

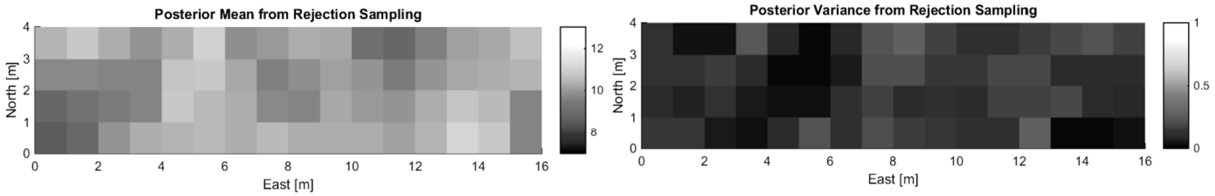

Figure 8 Average mean (left) and variance (right) maps of 290 posterior realizations accepted according to rejection sampling method

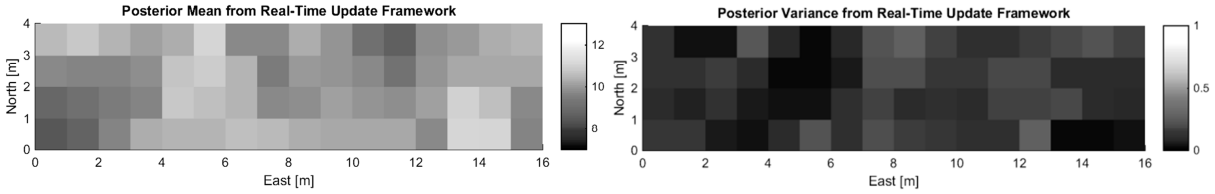

Figure 9 Average mean (left) and variance (right) maps of 1000 posterior realizations updated with real-time update framework

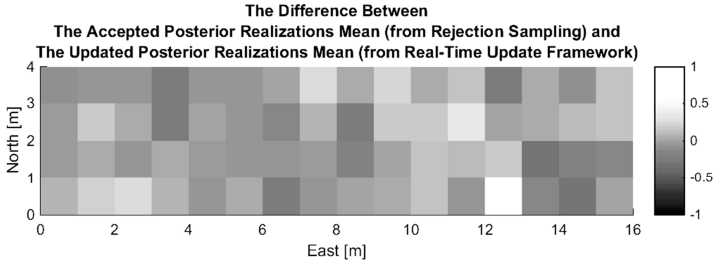

Figure 10 Difference map between the accepted posterior realizations from rejection sampling and updated posterior realizations from real-time update framework

In addition, MSE and BV graphs of mined, adjacent and indirect blocks from the accepted posterior models by rejection sampling (290) are given to provide the empirical and theoretical measures (Table 2). As mentioned in the previous section, both of the plots are prepared relative to the prior model in order to provide a good comparison. Again, each plot includes four bars, from left to right; prior model, mined blocks, adjacent blocks and indirect blocks.

Table 2 MSE and BV plots – Rejection Sampling

	Mined Blocks	Adjacent Blocks	Indirect Blocks
MSE	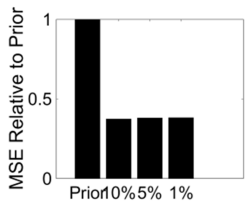	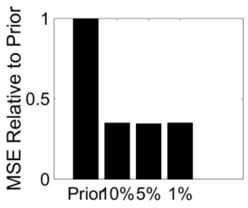	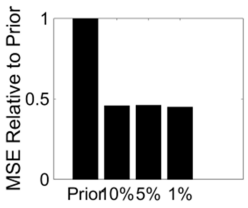
BV	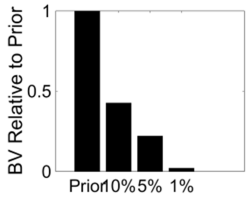	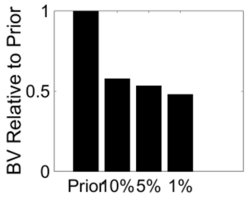	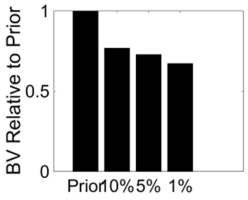

When BV values in Table 2 (MSE and BV plots of the accepted posterior models from rejection sampling) are compared to the ones in Table 1 (MSE and BV plots of the updated posterior realizations), similar trends are observed except relatively higher values in Table 2. The general behaviour of both tables is the increase of the block variance moving from mined blocks to indirect blocks, and the decrease of it when the sensor error is smaller. For the MSE values, an increase in the error rate is observable when moving from mined blocks to indirect blocks, yet the increase is not very significant. This is because the nature of rejection sampling does not take into account the weight of distances.

The mentioned similarities in the comparison of empirical error and theoretical variance of the accepted posterior realizations from rejection sampling and updated posterior realizations from real-time update framework, once again, indicate that the accepted models through rejection sampling are truly reflecting the updated models. This section concludes that the presented results validate the developed real-time updating framework and that it is a successful method for reaching the targets aimed for.

4 Application to a Full Scale Study

The aim of the case study which is presented here is to demonstrate the applicability of the developed framework in an industrial application.

As explained in Chapter 2, the defined study area is the Frimmersdorf lignite seam in Garzweiler mine, which is operated by RWE Power AG. The necessary data related to this research is provided by them. The following experiment is a benchmark in historical mined out area. The extraction sequence is reconstructed based on historical production data while KOLA data, which is assumed to represent the reality, is used for the evaluation of results.

4.1 Experiment Set-Up

First, the geological model (Figure 11) of the defined coal seam is created in a 32x32x1 m dimensioned block model based on the roof and floor information of the seam. Second, a 32x32x1 m dimensioned quality model that indicates the wet ash content in percentages is represented with 24 simulation and an estimation, based on the provided drill hole data. The simulated and estimated ash values are imported into previously defined coal seam. These are the first input file, the prior quality (ash) model.

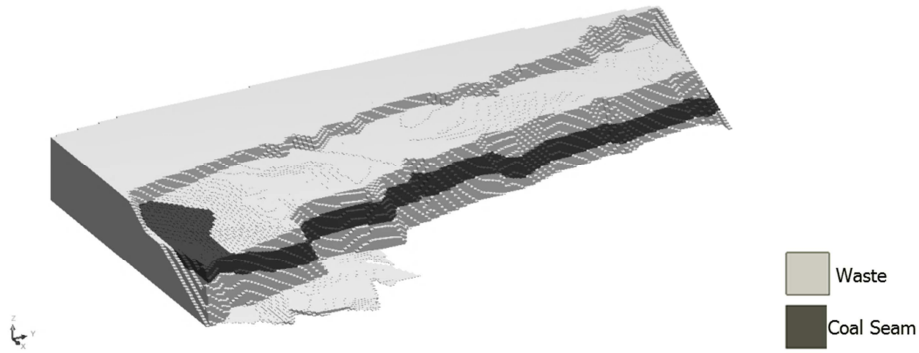

Figure 11 Geological model

Predicted measurements are obtained by averaging the simulated ash values from each simulation set, which falls into the defined production block boundaries. The online RGI sensor measurement data and KOLA data are provided for the time correspond to extracting. In order to determine the location of the received RGI and KOLA data, in other words to track back where the measured material comes from, the GPS data is matched with the measurement data based on the given timecodes. The located measurements in coal seams are then imported into the previously defined block model.

The second input file for the algorithm is written to a file containing the following information: the block ID, central block location (X, Y, Z coordinates), a series of real and predicted measurements.

A study bench produced for 15 days is defined by considering all the available data (topography, RGI, GPS and production data). Later, the study bench is divided into so-called “production blocks”. This was necessary to reproduce the excavated production blocks. The horizontal divisions (or production slices) are based on the movements of the excavator during production, which is based on GPS data. The vertical divisions are based on the changes in the Z coordinates in the GPS data. In the end, the defined production bench is divided into 28 blocks and 5 slices, which gives 140 production blocks. Once the study bench is divided both in vertical and horizontal, the production blocks are now ready to be updated.

The defined study bench is divided into blocks and their respective related block ID numbers are given in Figure 12. As a start the 2nd slice of the block number 1 is chosen to be updated, based on the KOLA measurements taken from that block. The series of updating experiments will continue until the 10th block. The update range is defined based on the variogram of the data as 450m in X and Y direction and 2.5m in Z direction. The expected improvements are marked as the circled neighbourhood area.

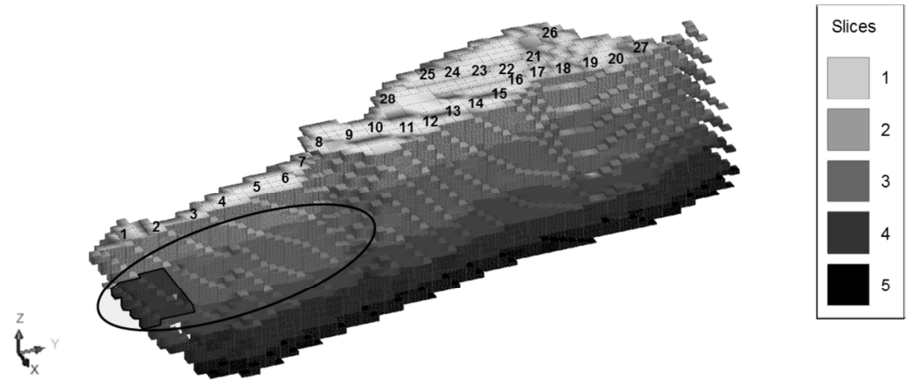

Figure 12 Production blocks

4.2 Results and Discussion

This section presents the results of the previously defined experiment. The added value of this application will also be discussed.

The first experiment uses the KOLA measurement, received from the 1st block's production, in order to update the neighbourhood blocks of the 1st block. Figure 13 illustrates the first experiment, where prior, posterior and measurement values are given. The averaged ash values from the prior simulation are represented with round dots and the related KOLA measurement values are given square marks. The light grey cloud of updated simulations covers the model uncertainty, while the long dashed line represents the average of the simulations.

Figure 14 to Figure 16 presents results of similar experiments, except the base of the update is moving forward from 1st block till the 9th block, as if the production moves. In each graph, the mined out area is indicated with an arrow. Among results of 7 experiments, only four of them (1st, 2nd, 4th and 7th) are presented here since they adequately represent the rest.

It is clearly seen from the Figure 13 that the average of the prior simulations dramatically underestimates the actual KOLA measurements. This happens because the prior simulations are created based on the coal samples in the drill holes, while the KOLA measurements measure higher ash values due to the sand intrusions in the coal seam. Integrating the KOLA measurement of the 1st block updates the first nine blocks to some higher values. As expected, the update effect decreases while moving away from Block 1.

Already from the second experiment (updating the ash values based on the measurement of the Block 2), the KOLA data is well covered by the range of uncertainty in the updated neighbourhood. While the integrated measurement number increases (experiment 2, 3, …, 7) it is observed that the uncertainty in the near neighbourhood gets slightly smaller and more of the actual KOLA measurements are captured by this uncertainty range.

The improvements from the very initial averaged prior simulation to the most recent updated simulations are clearly observable

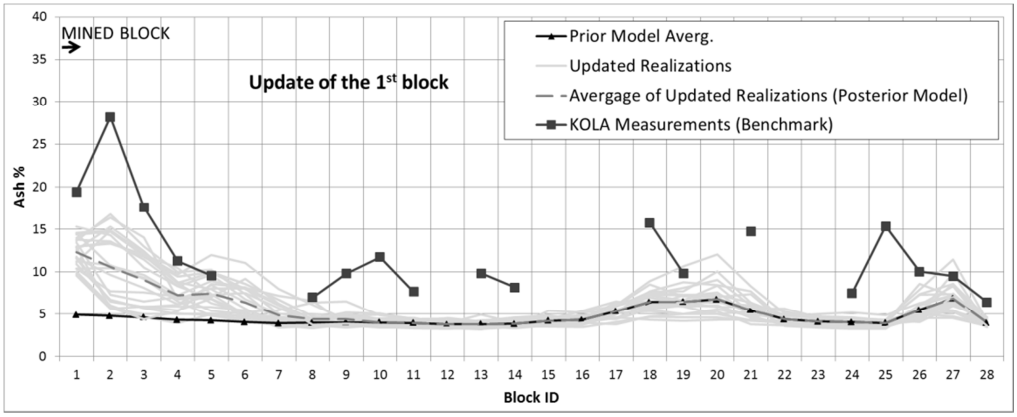

Figure 13 Experiment 1 - Updating: 2nd slice of the 1st block

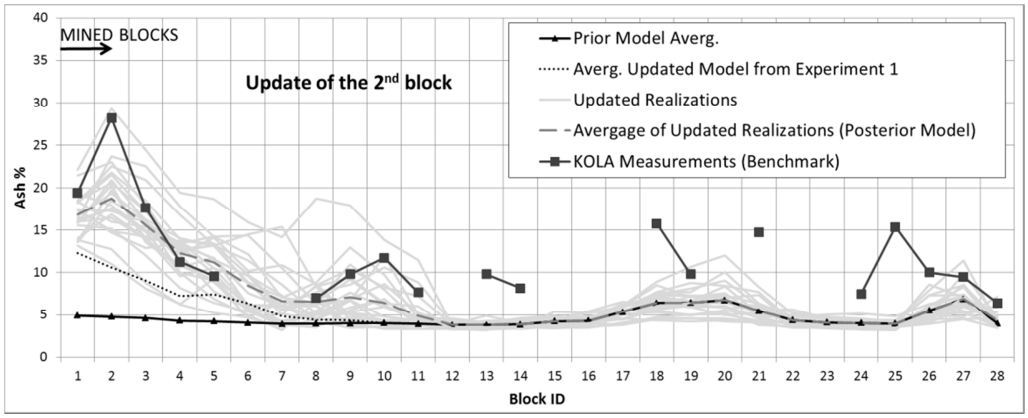

Figure 14 Experiment 2 - Updating: 2nd slice of the 2nd block

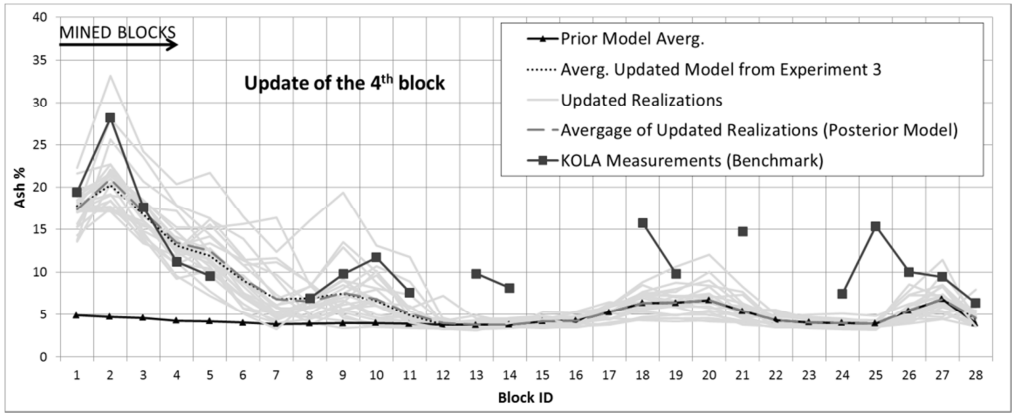

Figure 15 Experiment 4 - Updating: 2nd slice of the 4th block

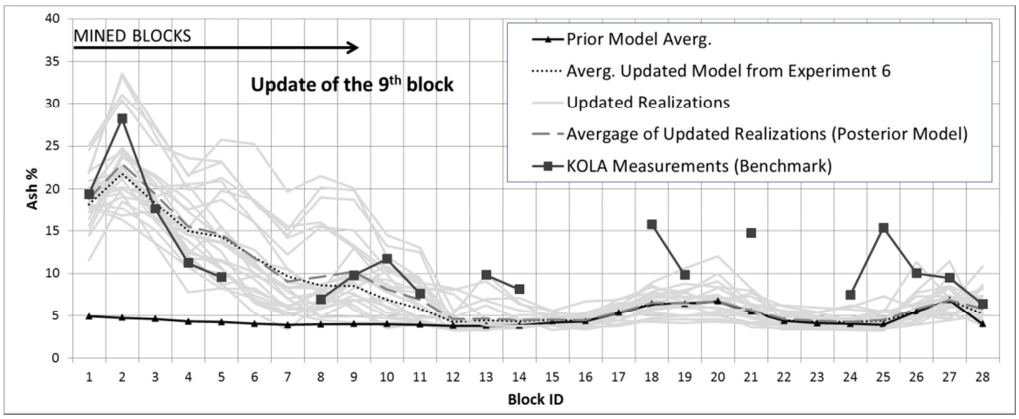

Figure 16 Experiment 7 - Updating: 2nd slice of the 9th block

The presented experiment demonstrated a resource model updating case study in a large open pit mining operation using the actual measurements, the so called KOLA data. The results have shown that the developed updating algorithm works well in a real-3D case.

Figure 17 gives the calculated MSE values for each performed experiment. Since this is a real case, the real block values are unknown. For this reason, the MSE compares the difference between estimated block value $\boldsymbol{Z}^*(\boldsymbol{x})$ and measured KOLA value (v). Once more, they are calculated relative to the prior averaged simulation. Figure 17 clearly indicates the improvements. The biggest improvement is observed on the first experiment, where the MSE value drops to 0.33 from 0.64. For the next experiments, the update is slightly smaller, yet observable. MSE values drop from 0.33 to 0.27 during the experiments between 2 and 7. This indicates in order of 70% improvement while integrating online measurement data into the resource model.

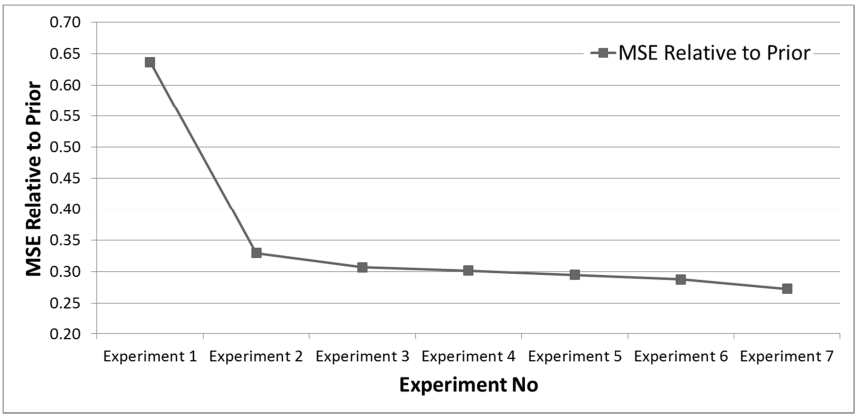

Figure 17 MSE Graph for performed experiments

5 Conclusions and Future Work

This study provides a tailored method for updating coal quality attributes in real-time and applying it in a real coal production environment.

This research allows for an improvement in predictions, leading to a potential increase of coal recovery and process efficiency by controlling the decisions continuously in a mining operation. The results from the full scale application validated the applicability of the method in a continuous mine environment and presented significant prediction improvements in the resource model.

Some limitations might be interpreting the results. A first potential limitation could be the quality of the provided data from RWE. For example, the accuracy and the representativeness of the received measurement data can highly effect the improvement of the results.

Future work will investigate the performance of the resource model updating framework by performing sensitivity analyses on main parameters, including the ensemble size, the neighbourhood size, localization strategies and the sensor precision.

The current research was limited to a case where only one excavator is operating. Another future project should apply a case study where two, three or four excavator are operating. This will require updating the coal quality parameters in different production benches based on one combined material measurement.

6 Acknowledgements

This research is a minor part of the Real-Time Reconciliation and Optimization in large open pit coal mines (RTRO-Coal) project and it is supported by Research Fund for Coal and Steel of European Union. RTRO-Coal, Grant agreement no. RFCR-CT-2013-00003.

7 References

Barbieri, R., & Schopf, P. (1982). *Oceanographic applications of the Kalman filter*. Greenbelt, Maryland 20771: Goddard Space Flight Center.

Barker, J. W., Cuypers, M., & Holden, L. (2000). *Quantifying uncertainty in production forecasts: Another look at the PUNQ-S3 problem.* Paper presented at the SPE Annual Technical Conference and Exhibition.

Bengtsson, L., Ghil, M., & Källén, E. (1981). *Dynamic meteorology: data assimilation methods* (Vol. 36): Springer New York.

Benndorf, J. (2015). Making use of online production data: Sequential updating of mineral resource models. *Mathematical Geosciences, 47*(5), 547-563.

Benndorf, J., Yueksel, C., Shishvan, M. S., Rosenberg, H., Thielemann, T., Mittmann, R., . . . Donner, R. (2015). RTRO–Coal: Real-Time Resource-Reconciliation and Optimization for Exploitation of Coal Deposits. *Minerals, 5*(3), 546-569.

Bertino, L., Evensen, G., & Wackernagel, H. (2002). Combining geostatistics and Kalman filtering for data assimilation in an estuarine system. *Inverse problems, 18*(1), 1.

Bertino, L., Evensen, G., & Wackernagel, H. (2003). Sequential data assimilation techniques in oceanography. *International Statistical Review, 71*(2), 223-241.

Bishop, C. H., Etherton, B. J., & Majumdar, S. J. (2001). Adaptive sampling with the ensemble transform Kalman filter. Part I: Theoretical aspects. *Monthly weather review, 129*(3), 420-436.

Brouwer, D., Naevdal, G., Jansen, J., Vefring, E., & Van Kruijsdijk, C. (2004). *Improved reservoir management through optimal control and continuous model updating.* Paper presented at the SPE Annual Technical Conference and Exhibition.

Buchardt, B. (1978). Oxygen isotope palaeotemperatures from the Tertiary period in the North Sea area.

Budgell, W. P. (1986). Nonlinear data assimilation for shallow water equations in branched channels. *Journal of Geophysical Research: Oceans, 91*(C9), 10633-10644. doi: 10.1029/JC091iC09p10633

Burgers, G., Jan van Leeuwen, P., & Evensen, G. (1998). Analysis scheme in the ensemble Kalman filter. *Monthly weather review, 126*(6), 1719-1724.

Chevalier, C., Emery, X., & Ginsbourger, D. (2014). Fast update of conditional simulation ensembles. *Mathematical Geosciences*, 1-19.

Cohn, S. E. (1997). An introduction to estimation theory. *JOURNAL-METEOROLOGICAL SOCIETY OF JAPAN SERIES 2, 75*, 147-178.

Daley, R. (1993). *Atmospheric data analysis*: Cambridge university press.

Evensen, G. (1994). Sequential data assimilation with a nonlinear quasi-geostrophic model using Monte Carlo methods to forecast error statistics. *Journal of Geophysical Research: Oceans (1978–2012), 99*(C5), 10143-10162.

Evensen, G. (1997a). Advanced data assimilation for strongly nonlinear dynamics. *Monthly weather review, 125*(6), 1342-1354.

Evensen, G. (1997b). *Application of ensemble integrations for predictability studies and data assimilation.* Paper presented at the Monte Carlo Simulations in Oceanography Proceedings' Aha Huliko'a Hawaiian Winter Workshop, University of Hawaii at Manoa.

Evensen, G., & Van Leeuwen, P. J. (1996). Assimilation of Geosat altimeter data for the Agulhas current using the ensemble Kalman filter with a quasigeostrophic model. *Monthly weather review, 124*(1), 85-96.

Evensen, G., & Van Leeuwen, P. J. (2000). An ensemble Kalman smoother for nonlinear dynamics. *Monthly weather review, 128*(6), 1852-1867.

Ghil, M., Cohn, S., Tavantzis, J., Bube, K., & Isaacson, E. (1981). Applications of estimation theory to numerical weather prediction *Dynamic meteorology: Data assimilation methods* (pp. 139-224): Springer.

Ghil, M., & Malanotte-Rizzoli, P. (1991). Data assimilation in meteorology and oceanography. *Advances in geophysics, 33*, 141-266.

Goovaerts, P. (1997). *Geostatistics for Natural Resources Evaluation*. New York Oxford: Oxford University Press.

Hager, H. (1986). Peat accumulation and syngenetic clastic sedimentation in the Tertiary of the Lower Rhine Basin, FR Germany. *Mem Soc Geol France NS, 149*, 51-56.

Haq, B. U., Hardenbol, J., & Vail, P. R. (1987). Chronology of fluctuating sea levels since the Triassic. *Science, 235*(4793), 1156-1167.

Heemink, A., & Kloosterhuis, H. (1990). Data assimilation for non-linear tidal models. *International journal for numerical methods in fluids, 11*(8), 1097-1112.

Hegstad, B. K., & Henning, O. (2001). Uncertainty in production forecasts based on well observations, seismic data, and production history. *SPE journal, 6*(04), 409-424.

Houtekamer, P. L., & Mitchell, H. L. (1998). Data assimilation using an ensemble Kalman filter technique. *Monthly weather review, 126*(3), 796-811.

Houtekamer, P. L., & Mitchell, H. L. (2001). A sequential ensemble Kalman filter for atmospheric data assimilation. *Monthly weather review, 129*(1), 123-137.

Houtekamer, P. L., Mitchell, H. L., Pellerin, G., Buehner, M., Charron, M., Spacek, L., & Hansen, B. (2005). Atmospheric data assimilation with an ensemble Kalman filter: Results with real observations. *Monthly weather review, 133*(3), 604-620.

Isaaks, E. H., & Srivastava, R. M. (1989). An introduction to applied geostatistics.

Jeong, C., Mukerji, T., & Mariethoz, G. (2011). *Iterative spatial resampling applied to seismic inverse modeling for lithofacies prediction.* Paper presented at the 81st Annual International Meeting, SEG, Expanded Abstracts.

Kalman, R. E. (1960). A New Approach to Linear Filtering and Prediction Problems *Transactions of the ASME–Journal of Basic Engineering, 82 (Series D)*, 35-45.

Klostermann, J. (1991). Die Wanderung der Kontinente. Grundlagen der Plattentektonik und die junge Beanspruchung der Niederrheinischen Bucht aus heutiger Sicht. *Natur und Landschaft am Niederrhein, 10*, 61-98, Krefeld.

Krige, D. (1951). *A Statistical Approach to Some Mine Valuation and Allied Problems on the Witwatersrand: By DG Krige.* University of the Witwatersrand.

Krige, D. (1981). *Lognormal-de Wijsian geostatistics for ore evaluation*: South African Institute of mining and metallurgy Johannesburg.

Liu, N., Betancourt, S., & Oliver, D. S. (2001). *Assessment of uncertainty assessment methods.* Paper presented at the SPE Annual Technical Conference and Exhibition.

Liu, N., & Oliver, D. S. (2003). Evaluation of Monte Carlo methods for assessing uncertainty. *SPE journal, 8*(02), 188-195.

Maybeck, P. S. (1979). Square root filtering. *Stochastic models, estimation and control, 1*, 368-409.

Miller, R. N. (1986). Toward the Application of the Kalman Filter to Regional Open Ocean Modeling. *Journal of physical oceanography, 16*(1), 72-86. doi: 10.1175/1520-0485(1986)016<0072:TTAOTK>2.0.CO;2

Nævdal, G., Johnsen, L. M., Aanonsen, S. I., & Vefring, E. H. (2005). Reservoir monitoring and continuous model updating using ensemble Kalman filter. *SPE journal, 10*(01), 66-74.

Nævdal, G., Mannseth, T., & Vefring, E. H. (2002). *Near-well reservoir monitoring through ensemble Kalman filter*. Paper presented at the SPE/DOE Improved Oil Recovery Symposium.

Sakov, P., & Bertino, L. (2011). Relation between two common localisation methods for the EnKF. *Computational Geosciences, 15*(2), 225-237.

Schäfer, A., Utescher, T., Klett, M., & Valdivia-Manchego, M. (2005). The Cenozoic Lower Rhine Basin–rifting, sedimentation, and cyclic stratigraphy. *International Journal of Earth Sciences, 94*(4), 621-639.

Schneider, H., & Thiele, S. (1965). Geohydrologie des Erftgebietes: Ministerium für Ernährung. *Landwirtschaft und Forsten, NRW, Düsseldorf*.

Sebacher, B., Hanea, R., & Heemink, A. (2013). A probabilistic parametrization for geological uncertainty estimation using the ensemble Kalman filter (EnKF). *Computational Geosciences, 17*(5), 813-832.

Stengel, R. (1994). Optimal Control and Estimation. New York: Dover Publications.

Tuan Pham, D., Verron, J., & Christine Roubaud, M. (1998). A singular evolutive extended Kalman filter for data assimilation in oceanography. *Journal of Marine systems, 16*(3), 323-340.

Verlaan, M., & Heemink, A. (1997). Tidal flow forecasting using reduced rank square root filters. *Stochastic Hydrology and Hydraulics, 11*(5), 349-368.

Wambeke, T., & Benndorf, J. (2015). *Data assimilation of sensor measurements to improve production forecasts in resource extraction*. Paper presented at the IAMG, Freiberg (Saxony) Germany.

Wambeke, T., & Benndorf, J. (2016). A Geostatistical Approach to Real-Time Reconciliation of the Grade-Control Model. *Mathematical Geosciences, submitted for publication*.

Webb, D. J. (1989). Assimilation of Data into Ocean Models. In D. T. Anderson & J. Willebrand (Eds.), *Oceanic Circulation Models: Combining Data and Dynamics* (Vol. 284, pp. 233-256): Springer Netherlands.

Zagwijn, W., & Hager, H. (1987). Correlations of continental and marine Neogene deposits in the south-eastern Netherlands and the Lower Rhine District. *Mededelingen van de Werkgroep voor Tertiaire en Kwartaire Geologie, 24*(1-2), 59-78.

Zhou, H., Gómez-Hernández, J. J., Hendricks Franssen, H.-J., & Li, L. (2011). An approach to handling non-Gaussianity of parameters and state variables in ensemble Kalman filtering. *Advances in Water Resources, 34*(7), 844-864.